

# **Novel CNC/Silica Hybrid as Potential Reinforcing Filler for Natural Rubber Compounds**

*Syed Danish Ali<sup>1,4</sup>, Marco Emilio Orlandi<sup>2</sup>, Luca Castellani<sup>3</sup>, Thomas Hanel<sup>3</sup>, Luca Zoia<sup>2\*</sup>*

<sup>1</sup> *Corimav-Pirelli, Department of Material Science, University of Milano-Bicocca, Via R. Cozzi 53,  
Milan, 20126, Italy*

<sup>2</sup> *Department of Earth and Environmental Sciences, University of Milano-Bicocca, Piazza della  
Scienza 1, Milan, 20126, Italy*

<sup>3</sup> *Pirelli Tyre SpA, Viale Sarca 222, Milan, 20126, Italy*

<sup>4</sup> *Nanoscience and Technology Department, National Centre for Physics, 45320, Islamabad,  
Pakistan*

*\* Corresponding Author: Luca Zoia, E-mail: luca.zoia@unimib.it.*

*Tel: (0039) 02-6448-2709.*

## **Abstract**

This work describes the development of a low-density, renewable and high reinforcing filler for natural rubber compounds. The cellulose nanocrystal (CNC) based CNC/Silica hybrid filler was synthesized by decorating the surface of CNCs with silica using a simple and efficient co-precipitation method. The properties of the prepared hybrid were investigated by Field emission scanning electron microscopy (FESEM), Fourier-transform infrared spectroscopy (FTIR), X-ray diffraction (XRD), nitrogen physisorption measurements, and Thermal Gravimetric Analysis (TGA). The surface area measurements of the hybrid before and after calcination at 600°C confirmed the core-shell structure of the prepared hybrid. Then, the prepared hybrid was incorporated in natural rubber (NR) using two different approaches, namely dry-mixing and co-precipitation. The prepared hybrid/NR compounds were vulcanized, and vulcanization characteristics were investigated. The dynamic and tensile mechanical properties of the hybrid/NR compounds were evaluated in both unvulcanized and vulcanized states. The co-precipitation method was found much more effective for homogeneous dispersion of the hybrid in rubber matrix. The CNC/Silica hybrid provided quite higher reinforcement to NR than reference silica however much lower density of the final compounds was obtained, so the prepared CNC/Silica hybrid can be used as potential low-density, high reinforcing filler in tire tread compounds.

**Keyword:** Cellulose NanoCrystals; Silica; Hybrid; Natural Rubber; Filler.

## 1. Introduction

Reinforcing fillers are the main component of rubber compounds which are added to improve the properties of elastomers. Carbon black and silica are the most commonly used reinforcing fillers in the tire industry due to their outstanding reinforcing effects [1–5]. The introduction of carbon black in tire compounds improves the strength, modulus, tear strength, and abrasion resistance [6,7]. Silica is also used in tire compounds to reduce the rolling resistance and heat build-up in-addition to high strength, modulus, and abrasion resistance [8–11]. Despite the high reinforcing effects of these fillers, there are some limitations of these fillers. Carbon blacks are mainly produced from non-renewable fossil fuels. Due to depletion and negative effects of fossil resources on the environment, there is a great demand for the development of materials from renewable resources. Moreover, the high densities of both carbon black ( $1.8 \text{ g/cm}^3$ ) and silica ( $2.0 \text{ g/cm}^3$ ) as compared to polymers ( $0.92 \text{ g/cm}^3$  for natural rubber) make the density of filled-rubber relatively high. Consequently, these fillers reverse the important property of the polymer materials, which is their low density. Furthermore, high energy and a long time are required for processing of silica. Considering these shortcomings, it is necessary to develop some alternative fillers with low density, eco-friendly, and renewable in nature to replace the traditional fillers used in the tire industry.

Cellulose nanocrystals (CNCs), an emerging class of extremely interesting bio-based nano-materials, have gained tremendous level of attention in both academic and industrial communities due to its fascinating physiochemical properties such as renewability, biodegradability, biocompatibility, environmental friendly, low density, high aspect ratio, high surface area, easy to process, and high mechanical properties [12–16]. Additionally, the axial Young's modulus of CNCs is equal to that of Kevlar but higher than steel. A theoretical study showed that a perfect crystal of cellulose has Young's modulus value of 167.5 GPa [17]. CNCs can be prepared from low-value lignocellulosic feedstock such as rice husk, *Arundo donax*, wheat straw, bagasse, etc. The abundant availability, chemical composition, and cost-effectiveness make the lignocellulosic biomass a promising feedstock to produce value-added products. In our previous study, we developed an integrated biorefinery process for the simultaneous recovery of CNCs, silica, lignin, and hemicellulose from rice husk and *Arundo donax* [18]. The CNCs and silica produced from these renewable lignocellulosic biomasses can be used as promising renewable reinforcing filler.

Based on the interesting properties of CNCs, the potential of CNCs to replace silica in rubber compounds was explored in this work by preparing a CNC/Silica hybrid. The hybrid organic/inorganic materials produced by combining organic and inorganic phases at the nanoscale

have attracted huge attention in the last few decades owing to their distinctive properties acquired by the synergistic combination of organic and inorganic components, with complementary properties [19–21]. The properties of these hybrid materials are not only the sum of the properties of their individual counterparts but the inner interface could also play an important role. Improved and unique properties of the hybrid materials allow the use of these materials in high-tech industrial applications [22]. Cellulose-based hybrid materials have been reported in the literature using cellulose or modified cellulose with different inorganic counterparts [23,24,33–37,25–32]. The presence of numerous hydroxyl groups on the surface of CNCs offers the possibility to chemically modify the surface and allow the use of CNCs as a template for loading the inorganic materials. Silica was selected to decorate the surface of CNCs as it can be produced from renewable resources and its commonly used as reinforcing filler in tire industry. The CNC/Silica hybrid will combine the properties of both CNCs and silica and could be ideal reinforcing filler for tire tread compounds. The resulting hybrid material will have a rod-like structure with high aspect ratio and lower density than silica. The silica layer on the surface of CNCs could show better compatibility with polymer matrix due to well-developed silica-silane technology and high aspect ratio hybrid particles will form strong percolation network to provide the high reinforcement to polymer matrix.

## **2. Experimental**

### **2.1 Materials**

Sodium hydroxide (NaOH), sulfuric acid (H<sub>2</sub>SO<sub>4</sub>), acetic acid, cetyltrimethylammonium bromide (CTAB), ethanol, and bis[3-(triethoxysilyl)propyl]tetrasulfide (TESPT) were purchased from Sigma-Aldrich. CNCs used in this work were obtained in the form of aqueous suspension (11.5-12.5%, w/w) from Cellulose Lab, Canada. The length of the CNCs ranges between 150 to 200 nm, width from 5 to 20 nm and the density of dried CNCs powder was 1.5 g/cm<sup>3</sup>. Natural rubber (SIR-20 grade) was purchased from Astlett and natural rubber latex was supplied by Von Bundit, Thailand with solid contents of 60% (w/w). High dispersible silica Ultrasil VN3 was from Evonik, soluble sulfur was from Zolfoindustria, zinc oxide was from Zincolossidi, stearic acid was from Sogis, N-cyclohexyl-2-benzothiazylsulfenamide (CBS) was from Zolfoindustria, 2,2,4-trimethyl-1,2-dihydroquinoline (TMQ) was from Sovchem, and N-(1,3-Dimethylbutyl)-N'-phenyl-p-phenylenediamine (6PPD) was obtained from Eastman.

### **2.2 Methods**

#### **2.2.1 CNC/Silica Hybrid Synthesis**

The CNC/Silica hybrid (CSH) was synthesized by co-precipitation method. The procedure used here is the modification of method used for the precipitation of silica by Dokter and Tjburg [38]. Initially,

a sodium silicate solution was prepared by adding 7 g of silica and 2.8 g NaOH in 90 ml of distilled water in a round bottom flask and reaction mixture was stirred at 300 rpm for 1 h at 80°C. A clear solution was obtained at the end. In another three neck round bottom flask, about 5 g (42 g CNC suspension 12% w/w) of CNC and 0.8 g of CTAB was added in 450 ml of distilled water. This reaction mixture was stirred for 30 min and the temperature was maintained at 75-85°C. This temperature was maintained throughout the reaction. The initially prepared sodium silicate solution was added to the above CNCs solution at a rate of 0.67 ml/min for about 90 min. During the addition of sodium silicate solution, the sulfuric acid (15 % w/w) was added simultaneously to maintain the pH of the reaction mixture at 9.2-9.4. After 90 min of reaction, the dosing of sodium silicate solution and sulfuric acid were stopped and the reaction mixture was allowed to stirring for 15 min. Then, sulfuric acid was added again in 10 min so that the pH was lowered to 7.5. The sodium silicate solution was dosed again at a rate of 0.67 ml/min for next 45 min and the pH was maintained at 7.3-7.6 by simultaneous addition of sulfuric acid (15%, w/w). After 45 min of reaction, sulfuric acid (15%, w/w) was dosed again in 20 min so that the pH was lowered to 4. The resulting precipitated hybrid was obtained after centrifugation at an acceleration of 3200 g for 10 min, repeatedly washed with distilled water until all CTAB was removed and freeze dried.

### **2.2.2 Characterizations of CNC/Silica Hybrid**

The ATR-FTIR spectra of CNC, Silica and CHS were performed with a Nicolet iS10 spectrometer (Thermo Scientific) equipped with an iTR Smart device (total scan 32, range 4000-800  $\text{cm}^{-1}$ , resolution 1  $\text{cm}^{-1}$ ).

The surface morphology and dimensions of the prepared hybrid were investigated by Field Emission Scanning Electron Microscopy (FESEM). The sample for analysis was prepared by dispersing a small amount of prepared hybrid in ethanol and sonicated for 15 min. A drop of the suspension was placed on a silicon substrate and dried in air. The FESEM analysis was performed using Zeiss UltraPlus FESEM operating at 7.0 kV and the working distance between 3.5 and 4 mm. The images were recorded at different magnifications.

Total surface area, micropores area, and micropore volume were measured by nitrogen physisorption using a Quantachrome Autosorb-1 apparatus according to BET and t-plot methods. The samples were evacuated at 200°C for 16 h before the analysis.

Thermal Gravimetric analysis (TGA) of the prepared hybrid was performed using Mettler Toledo TGA1 instrument. Few milligrams of the sample were placed in an open crucible pan and heated from 30°C to 800°C in a nitrogen atmosphere with nitrogen flow rate of 60 ml/min.

Powder XRD analysis of CNCs, silica, and the CHS was performed using the X'Pert PRO diffractometer from PANalytical Company, using Cu K $\alpha$  (1.54 Å) as an X-ray source. The operating voltage and current were kept at 40 kV and 30 mA respectively.

### 2.2.3 Rubber Compounding

The natural rubber (NR) compounds of CSH and reference silica were prepared by two methods; dry mixing and co-precipitation. Formulation of the prepared compounds in parts per hundred parts of rubber (PHR) is shown in Table 1. For each method, a reference silica compound was prepared. The Dry-CSH and Dry-Silica represent the CSH compound and reference silica compound prepared by dry mixing, respectively. The Co-CSH and Co-Silica represent the CSH compound and reference silica compound prepared by co-precipitation method, respectively.

Ingredients	Dry-Silica	Dry-CSH	Co-Silica	Co-CSH
NR	100	100	-	-
Silica	30	-	-	-
CSH	-	30	-	-
NR/Silica Masterbatch	-	-	130	-
NR/CSH Masterbatch	-	-	-	130
TESPT	2.4	2.4	2.4	2.4
Soluble Sulfur	2	2	2	2
Zinc Oxide	5	5	5	5
Stearic Acid	2	2	2	2
CBS	2	2	2	2
TMQ	1	1	1	1
6PPD	1.5	1.5	1.5	1.5

**Table 1.** Formulation of the prepared rubber compounds in PHR

In the dry mixing, the rubber compounds were prepared by mixing all the ingredients through mechanical blending using the Brabender internal mixer (chamber volume 50 mL, 0.9 fill factor) using the procedure described in Table 2. In co-precipitation method, the masterbatches of NR with fillers were initially prepared. To prepare NR/filler masterbatches, calculated amount of filler according to the final concentration (e.g. 9.76 g of hybrid for 30 PHR of filler contents) was added to 50 ml of water and mechanically stirred for 1 h to make homogeneous dispersion. The dispersion was added to 54.5 g of 60% (w/w) natural rubber latex. The emulsion was stirred for 1 h at room temperature. Then, the emulsion was coagulated by progressive addition of the acetic acid solution (10% v/v). The coagulated rubber was reduced to a thin sheet using a two-roll mill and washed with distilled water until neutral pH was reached. The thin sheets of masterbatch were dried under vacuum

at 40°C until constant weight. The obtained masterbatches were mixed with other ingredients (silane, vulcanizers, and antioxidants) using Brabender internal mixer using the procedure given in Table 2.

	<b>Time (min)</b>	<b>RPM</b>	<b>Temp (°C)</b>	<b>Operation</b>
<i>Step 1</i>	0	60	60	Loaded the masterbatch/NR
	3	60	60	Added silane/filler
	7	60	60 → 140	Raised the temperature
	8	60	140	Added stearic acid and zinc oxide
	10	60	140	Unloading
<i>Step 2</i>	0	60	60	Loaded compound from step-1
	4	60	60	Added vulcanizers and antioxidants
	9	60	60	Unloading the compound

**Table 2.** Mixing procedure of rubber compounds

The effect of filler contents on the properties of the natural rubber compounds was studied by preparing the compounds with 20, 30 and 40 PHR of filler contents using the formulation shown in Table 3.

<b>Ingredients</b>	<b>Silica-20</b>	<b>Silica-30</b>	<b>Silica-40</b>	<b>CSH-20</b>	<b>CSH-30</b>	<b>CSH-40</b>
NR	100	100	100	-	-	-
Silica	20	30	40	-	-	-
Masterbatch NR(100PHR)+CSH(20PHR)	-	-	-	120	-	-
Masterbatch NR(100PHR)+CSH(30PHR)	-	-	-	-	130	-
Masterbatch NR(100PHR)+CSH(40PHR)	-	-	-	-	-	140
TESPT	1.6	2.4	3.2	1.6	2.4	3.2
Soluble Sulfur	2	2	2	2	2	2
Zinc Oxide	5	5	5	5	5	5
Stearic Acid	2	2	2	2	2	2
CBS	2	2	2	2	2	2
TMQ	1	1	1	1	1	1
6PPD	1.5	1.5	1.5	1.5	1.5	1.5

**Table 3.** Formulation in PHR of the prepared compounds with different filler content

## **2.4 Characterization of Rubber Compounds**

The density of the rubber compounds was measured on few grams of the rubber compounds using Micromeritics AccuPy C 1330 helium pycnometer.

The dispersion of the filler in the rubber matrix was analyzed by Optical microscope. The analysis was performed on a freshly cut sample of vulcanized rubber compounds. The sample was freeze-dried in liquid nitrogen and test sample to 1 micron was cut by Leica RM2165 microtome. The analysis was performed using Leica DM4000 M microscope with a 100x objective. Images of the surface of the samples were recorded.

The vulcanization curves of the prepared compounds were recorded using a Moving Die Rheometer (RPA 2000, Alpha Technologies). The measurements were performed at a temperature of 150°C, 4.3 bar pressure, running time of 30 min, and rotor frequency of 1 Hz.

Dynamic mechanical analysis of both unvulcanized and vulcanized compounds were performed by using Rubber Process Analyzer (RPA 2000, Alpha Technologies) working in a shear stress mode. The strain sweep measurements were performed from 1 to 100 % strain at 70°C and frequency of 1 Hz.

For tensile mechanical analysis, the samples were pressed in 2 mm thick sheets by a two-roll mill and vulcanized in a hydraulic press under a pressure of 4.3 bar at 150°C for 30 min. The vulcanized samples were conditioned in the measuring environment for 24 h. Samples for analysis were prepared by die-cutting the vulcanized sheets in five dumbbell-shaped specimens of standard dimensions. The measurements were performed according to ISO 37 and UNI 6065 standards by using Zwick/Roell tensile testing machine. The stress-strain curves were recorded by progressive straining of samples. The data reported in the result and discussion section are the mean of 5 analyses.

## **3. Results and Discussion**

### **3.1 CNC/Silica Hybrid Synthesis**

The CNC/Silica hybrid was synthesized by decorating the surface of CNCs with the layer of silica nanoparticles. The CNCs obtained through sulfuric acid hydrolysis process carry negative charges due to the attachment of sulfate groups on the surface of CNCs. Therefore, cetyltrimethylammonium bromide (CTAB) was added during the synthesis of the hybrid. Since CTAB is a cationic surfactant, it can be adsorbed or aligned on the surface of CNCs and could act as a bridge of electrostatic attractions between the CNCs surface and silica solution and facilitate the deposition of silica on the CNCs surface [39]. CTAB functioned as nuclei center for the growth of silica particles and played an important role in the synthesis of core-shell structure of the CNC/Silica hybrid.

FTIR analysis was performed to confirm the synthesis of CNC/Silica hybrid and it was performed in comparison with pure CNCs and silica. FTIR spectra of CNCs, silica and CNC/Silica hybrid are shown in Fig. 2. The FTIR spectrum of CNC/Silica hybrid shows the characteristics peaks of both CNCs and silica. The peaks appeared at  $1080\text{ cm}^{-1}$  and  $800\text{ cm}^{-1}$  in the spectrum of silica correspond to the Si-O-Si asymmetric and symmetric stretching vibrations [40]. The stretching vibration of the C-O-C or Si-O-C bonds also appeared at  $1100\text{-}1000\text{ cm}^{-1}$  and overlapped with the band of silica in the same spectral region [41,42]. Furthermore, it was also observed that the characteristic peaks of the CNCs at  $1155$ ,  $1105$  and  $900\text{ cm}^{-1}$  corresponding to the stretching vibration of the C-C bond, C-O-C glycosidic ether bond, and C-O-C cellulose  $\beta$ -glycosidic linkage, respectively, were detected. It is worth noticing that the signal of CTAB (easily detectable at  $3000\text{-}2900\text{ cm}^{-1}$ ) was not observed indicating the efficient washout of the surfactant after the synthesis.

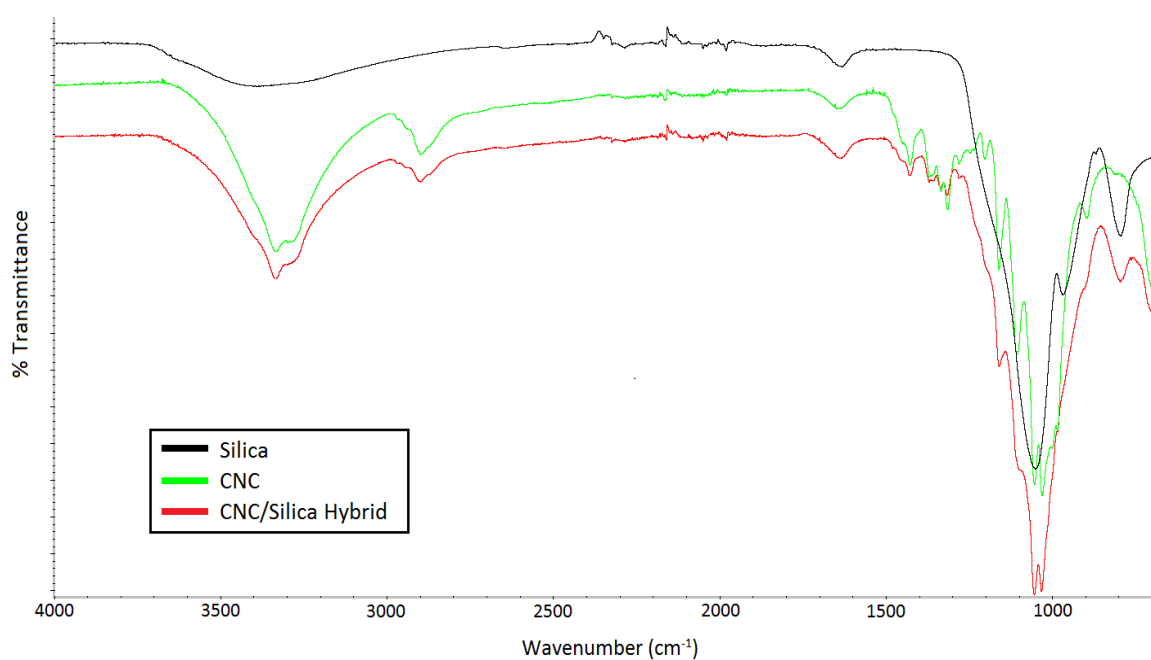


**Figure 2.** FTIR spectra of CNCs, silica and CNC/Silica hybrid.

The morphology of the prepared CNC/Silica hybrid was studied by FESEM analysis. The FESEM images of the hybrids at different magnifications are shown in Fig. 3. A clear rod-like morphology of the CNC/Silica hybrid can be seen from these images, which shows that silica was successfully deposited on the surface of CNCs maintaining the original rod-like morphology of CNCs. The width of these rod-like hybrid particles ranges between 20 to 35 nm and length between 150-200 nm. These results seem to confirm the synthesis of core-shell structured CNC/Silica hybrid.



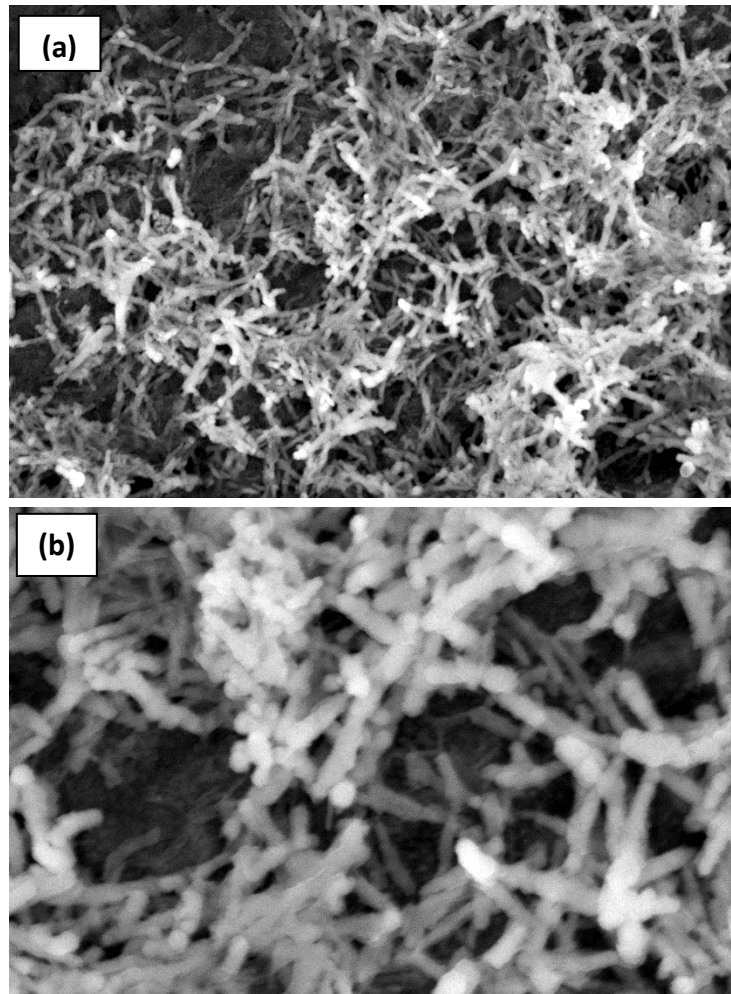


**Figure 3.** FESEM images of prepared hybrid at 31.75 KX (a) and 100.00 KX (b) magnification.

The total surface area, external surface area, micropores area and micropores volume of the CSH hybrid were measured before and after calcination at 600°C for 3 h. The values are reported in Table 4. The total surface area of the pristine hybrid was 138.0 m<sup>2</sup>/g, which was increased to 389.92 m<sup>2</sup>/g after calcination, which is due to the increase of micropores area. The micropores volume of the hybrid was also increased significantly after calcination. It was proposed that the CNCs functioned as template in the synthesis of CNC/Silica hybrid, the removal of CNCs through calcination created the silica nanotubes with micro-channel or micropores. Due to the creation of this micro-channel, the micropores area and micropores volume were significantly increased. These results support our proposal of formation of the core-shell structure of the CNC/Silica hybrid and are in good agreement with the FESEM results.

Sample	Total Surface Area (m <sup>2</sup> /g)	External Surface Area (m <sup>2</sup> /g)	Micropores Area (m <sup>2</sup> /g)	Micropores Volume (cm <sup>3</sup> /g)
Hybrid	138.07	109.17	28.89	0.009775
Hybrid (Calcined)	389.92	115.98	272.93	0.125803

**Table 4.** Surface area and pore volume of the hybrid before and after calcination.

The thermal gravimetric analysis of the CNC/Silica hybrid was performed not only to measure the CNCs and silica contents but also to study the thermal stability of the prepared hybrid during the processing of the rubber compounds. It is important that the material must be thermally stable during the mixing and vulcanization process. Typically, the vulcanization process is carried out at temperatures of 140-170°C for 10-30 min, so the material should withstand the high processing temperatures during this process. Therefore, the TGA analysis was performed in three steps with two isothermal conditioning periods, each one lasting for 15 min. The first step performed at 30-80°C showed a weight loss of about 3.7% due to the loss of adsorbed water. The presence of physisorbed water is very important and reactivity of silane with silica is strongly influenced by the physisorbed water [28–30]. The second step performed at 80-170°C was carried out to access the thermal stability of the hybrid during the vulcanization process. The results showed a high thermal stability of the hybrid and only 0.44% weight loss was observed which is due to the loss of water produced by the condensation of silanol groups on the silica surface. The third step performed between 170-800°C was carried out to determine the loading of silica on CNCs surface. The prepared hybrid was thermally stable up to 280°C, and then the CNCs started to decompose. From the results, it was calculated that the prepared CNC/Silica hybrid contains about 45% of CNCs content and about 55% of silica content.

The crystalline structure of the prepared hybrid was investigated by XRD. The XRD patterns of CNCs, silica and prepared hybrid are shown in Fig. 4. Broad peak observed in the XRD pattern of silica centered at 2-theta = 22.2° shows the amorphous structure of the silica. The CNCs showed high crystallinity and XRD pattern of CNCs showed the characteristics peaks of the cellulose I $\beta$  and cellulose II. Peaks observed at 2-theta = 14.8°, 16.5°, 22.5°, and 34.6° correspond to the cellulose I $\beta$  and two other peaks observed at 12.2° and 20.2° correspond to the cellulose II. The XRD pattern of the hybrid displayed the combined reflection of CNCs and silica. The peaks observed at 2-theta = 20.2° and 22.5° correspond to the characteristic peaks of CNCs combined with the broad peak of silica. The crystallinity of the hybrid was reduced due to the presence of amorphous silica. A sharp small peak observed at 2-theta = 31.9° is due to sodium sulfate, formed during the hybrid synthesis. The presence of a small percentage of sodium and sulfur was confirmed by the elemental analysis (not reported).

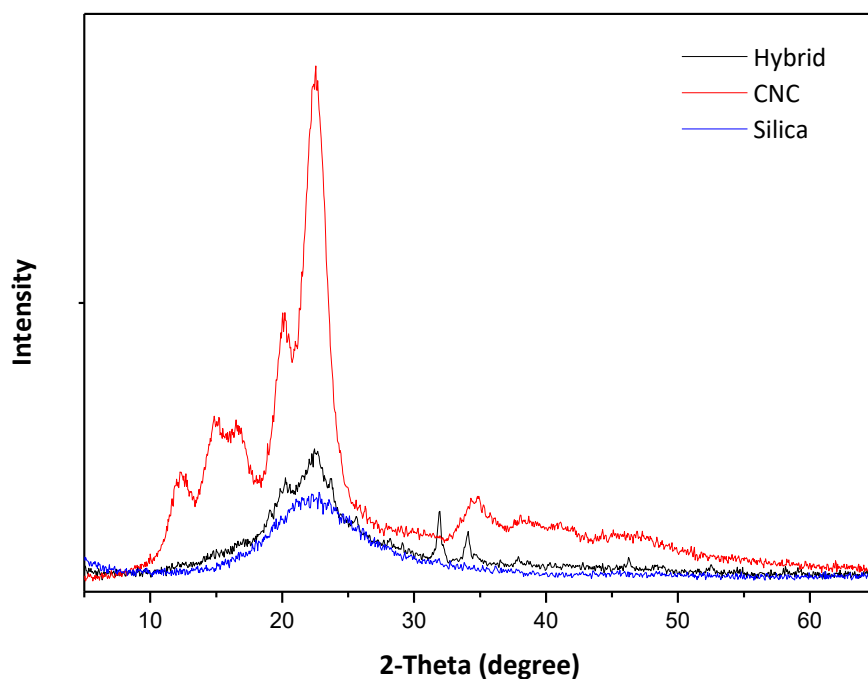


**Figure 4.** XRD patterns of silica, CNCs, and the hybrid.

### 3.7 Rubber Compounds of CNC/Silica Hybrid

#### 3.7.1 Properties of Rubber Compounds

Two different methods used for the preparation of rubber compounds demonstrated a significant effect on the dispersion of fillers in the rubber matrix. The dispersion of the filler in polymer matrix plays an important role in determining the reinforcement capability of the filler. The optical microscope images of the prepared rubber compounds, showing the filler dispersion in the rubber matrix, are shown in Fig. 5. Silica and hybrid agglomerates can be clearly seen as white dots and carbon black as black dots. A high agglomeration of the hybrid was observed in the dry-mixed compound while the hybrid was homogeneously dispersed in the co-precipitated compound. During the drying process of hybrid, the high surface area and high aspect ratio lead to aggregation of hybrid nanoparticles. The dry mixing process of this hybrid with natural rubber in the internal mixer was not able to break down these aggregates and resulted in the poor dispersion of hybrid in the rubber matrix. On the other hand, during the co-precipitation method, the hybrid suspension was not dried and mixed as such with natural rubber latex. This process resulted in a very high dispersion of hybrid in the rubber matrix. Processing method does not have considerable influence on silica dispersion, as commercial high dispersible silica was used, is the study. Therefore, silica was highly dispersed in both methods, but slightly better dispersion was observed in compound prepared through the co-precipitation method.

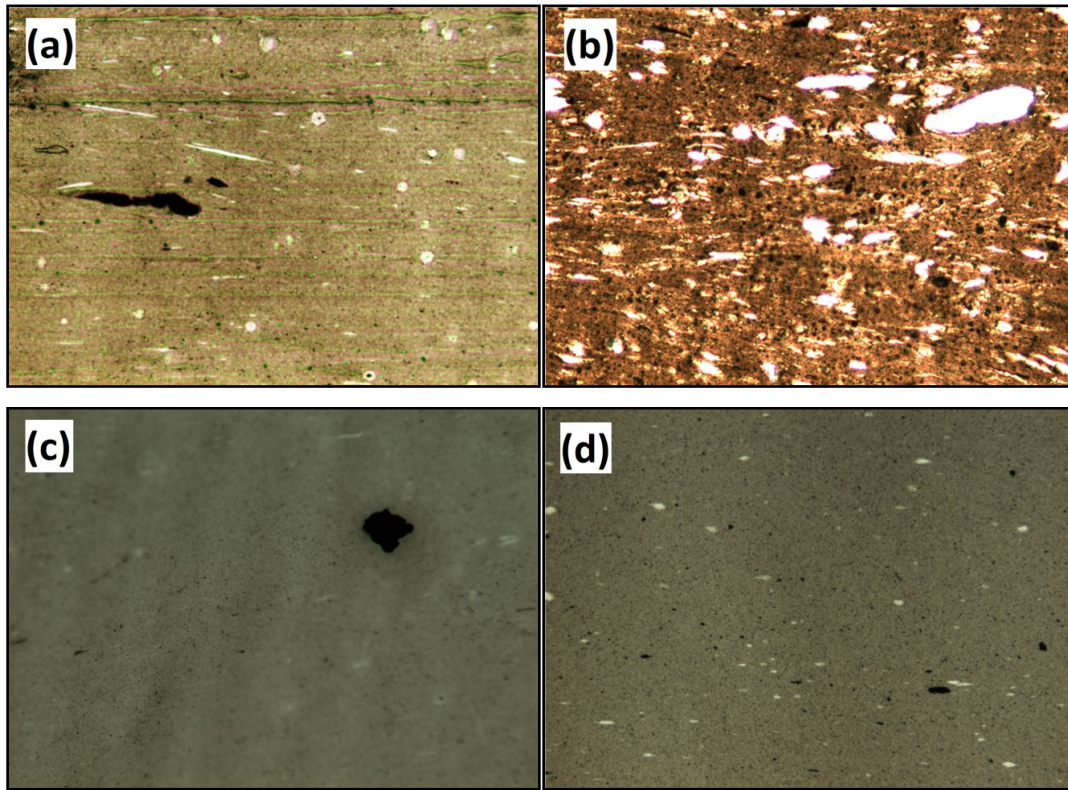


**Figure 5.** Optical microscope images of (a) Dry-Silica (b) Dry-CSH (c) Co-Silica (d) Co-CSH compounds at magnification of x100.

The vulcanization characteristics, such as scorch time ( $T_{S2}$ ), optimum curing time ( $T_{90}$ ), minimum ( $M_L$ ), and maximum ( $M_H$ ) values of torques of the prepared compounds, were calculated from vulcanization curves. Table 5 shows the vulcanization parameters of the prepared compounds. The hybrid has almost the same vulcanization behavior irrespective of the preparation method. However, the behavior of hybrid is quite different from its corresponding reference silica compound. The hybrid has a significant effect on the scorch time and optimum curing time of the prepared compounds.  $T_{S2}$  and  $T_{90}$  of the hybrid compounds are quite lower than the silica compounds.  $T_{S2}$  and  $T_{90}$  are the two important parameters of vulcanization process and represent the time of initiating crosslinking reactions and the time required for the optimum value of curing. These two parameters determine the curing rate index (CRI) which is proportional to the average slope of cure rate in the steep region [ $CRI = 100 / (T_{90} - T_{S2})$ ] [43]. Vulcanization process of hybrid compounds was much faster and showed quite higher values of CRI than the corresponding silica compounds. Hence, these results show that the hybrid accelerated the process of vulcanization and reduced the time of initiating the curing process and time of curing and increased the curing rate of the rubber compounds. This is due to the fact that the silica could adsorb the vulcanizers which lead to the slowdown of vulcanization process

[44]. Two other important parameters of the vulcanization process are  $M_L$  and  $M_H$ .  $M_L$  is directly related to the viscosity of the compounds in unvulcanized state at the test temperature. It was observed from the results that the  $M_L$  values are almost similar for all the compounds. This implies that the hybrid did not have a significant effect on the viscosity of the unvulcanized compounds.  $M_H$  predominantly depends on the crosslinking density and reinforcement of filler in the rubber matrix [45]. The  $M_H$  values of the hybrid compounds are much higher than the corresponding reference silica compounds. This observation is attributed to the increased crosslink density. The degree of crosslinking, calculated as the difference between the maximum and minimum torques ( $\Delta M = M_H - M_L$ ), is quite higher for the hybrid compounds than silica compounds. This showed a higher reinforcement effect of the hybrid than silica [46,47]. These results showed that the hybrid has improved vulcanization characteristics than silica and preparation method of rubber compounds did not have a significant influence on vulcanization characteristics.

Parameter	Dry-Silica	Dry-CSH	Co-Silica	Co-CSH
$T_{s2}$ (min)	7.33	4.8	7.83	4.46
$T_{90}$ (min)	12.87	9.02	13.92	9.28
CRI ( $\text{min}^{-1}$ )	18.05	23.70	16.42	20.75
$M_L$ (dNm)	1.91	1.86	1.93	2.06
$M_H$ (dNm)	14.37	17.64	14.38	17.71
$\Delta M$ (dNm)	12.46	15.78	12.45	15.65

**Table 5.** Vulcanization parameters of the prepared compounds.

Dynamic mechanical analysis of the prepared rubber compounds was performed in shear stress mode before and after vulcanization. The effect of the hybrid as reinforcing filler in comparison with silica on the dynamic mechanical properties, such as storage modulus and  $\tan \delta$  was studied. The effect of the processing methods of rubber compounds on these properties was also investigated. The strain sweep curves of the unvulcanized and vulcanized compounds are shown in Fig. 6. All the compounds either unvulcanized or vulcanized showed viscoelastic behavior, characterized by the typical non-linear dependence of storage modulus  $G'$  on the applied dynamic strain. This strain softening is due to the breakdown of the filler network upon oscillatory shear. Based on this widely accepted mechanism, the modulus at low strain ( $G'_0$ ) is the representative of filler-filler interactions. The modulus at high strain ( $G'_\infty$ ) comes from three strain independent contributions; polymer network, hydrodynamic effect and in-rubber structure (filler-polymer interactions). The higher  $G'_0$  values for the hybrid compounds than the silica compounds demonstrated the stronger filler-filler interactions and higher reinforcement effect. The strong filler network of hybrid is attributed to the high aspect

ratio of the hybrid particles which enhanced the possibility to make strong hydrogen bonding between particles. Furthermore, the  $G'_{\infty}$  is higher for Co-CSH compound than other hybrid and silica compounds in unvulcanized and vulcanized states. At high strain, only different filler-rubber interactions could differentiate the dynamic mechanical characteristics of the compounds, as the filler particles are supposed to be not mutually interacting. This high value of  $G'_{\infty}$  for Co-CSH compound is due to better dispersion and the large contact area between the anisotropic hybrid particles and polymer. The behavior of the hybrid was strongly influenced by the compound preparation method. In the unvulcanized compounds, the Dry-CSH showed much higher  $G'_{\circ}$  value (high filler-filler interactions) than Co-CSH. This is due to the poor dispersion of the hybrid during the dry-mixing process which increased the interaction between the hybrid aggregates and resulted in high stiffness of the compound at low strain. It should be noted that a high value of  $G'_{\circ}$  does not mean the filler network is percolated throughout the specimen. Local subnetworks also contribute to the  $G'_{\circ}$  value and yield a Payne effect [48]. The hybrid prepared through the co-precipitation method was efficiently dispersed, which resulted in lower filler-filler interactions but higher filler-polymer interactions, as evident by the higher value of modulus for Co-CSH at high strain. Furthermore, as shown in Table 6, the Payne effect of the Co-CSH compound is much lower than Dry-CSH compound which shows a high filler networking capability of the hybrid in dry mixing. On the other hand, after the vulcanization of hybrid compounds, the Co-CSH has higher  $G'_{\circ}$  than Dry-CSH but similar  $G'_{\infty}$  values. Due to the high degree of crosslinking of hybrid compounds, the difference of filler-polymer interactions between the two hybrids was diminished and showed similar modulus at high strain. The higher  $G'_{\circ}$  for Co-CSH could be due to the flocculation of the filler during the vulcanization process. At high temperature during the vulcanization, the low viscosity of the polymer enhances the mobility of the filler, which tends to aggregate and make strong filler network. As the hybrid was already agglomerated in the dry-mixed compound, filler network did not contribute significantly to the increase of modulus, as no considerable change in Payne effect was observed after vulcanization. The increase in modulus after the vulcanization is due to the formation of the cross-linked polymer network. A similar trend was observed in the case of silica compounds but the difference was very small because the silica was well dispersed in both compounds. A small difference in Payne effect of the two compounds was observed and Co-Silica compound showed lower Payne effect than Dry-Silica compound which is probably due to the better dispersion of silica by co-precipitation, which resulted in lower filler-filler but higher filler-polymer interactions. In the vulcanized compounds, two silica compounds showed the same behavior against increasing strain but a parallel shift of the curve of Co-Silica to lower values of the modulus. It was supposed that this parallel shift in the  $G'$  value was caused by a strain-independent contribution. As the filler and crosslink density of the two

compounds are same, so this shift can only be due to in-rubber structure [48]. In-rubber structure is the measure for the rubber entrapped between the filler, term as occluded rubber, which is shielded from deformation and enhance the effective filler loading. During the co-precipitation, the structure of the silica was slightly lowered which resulted in a parallel shift to lower modulus values.

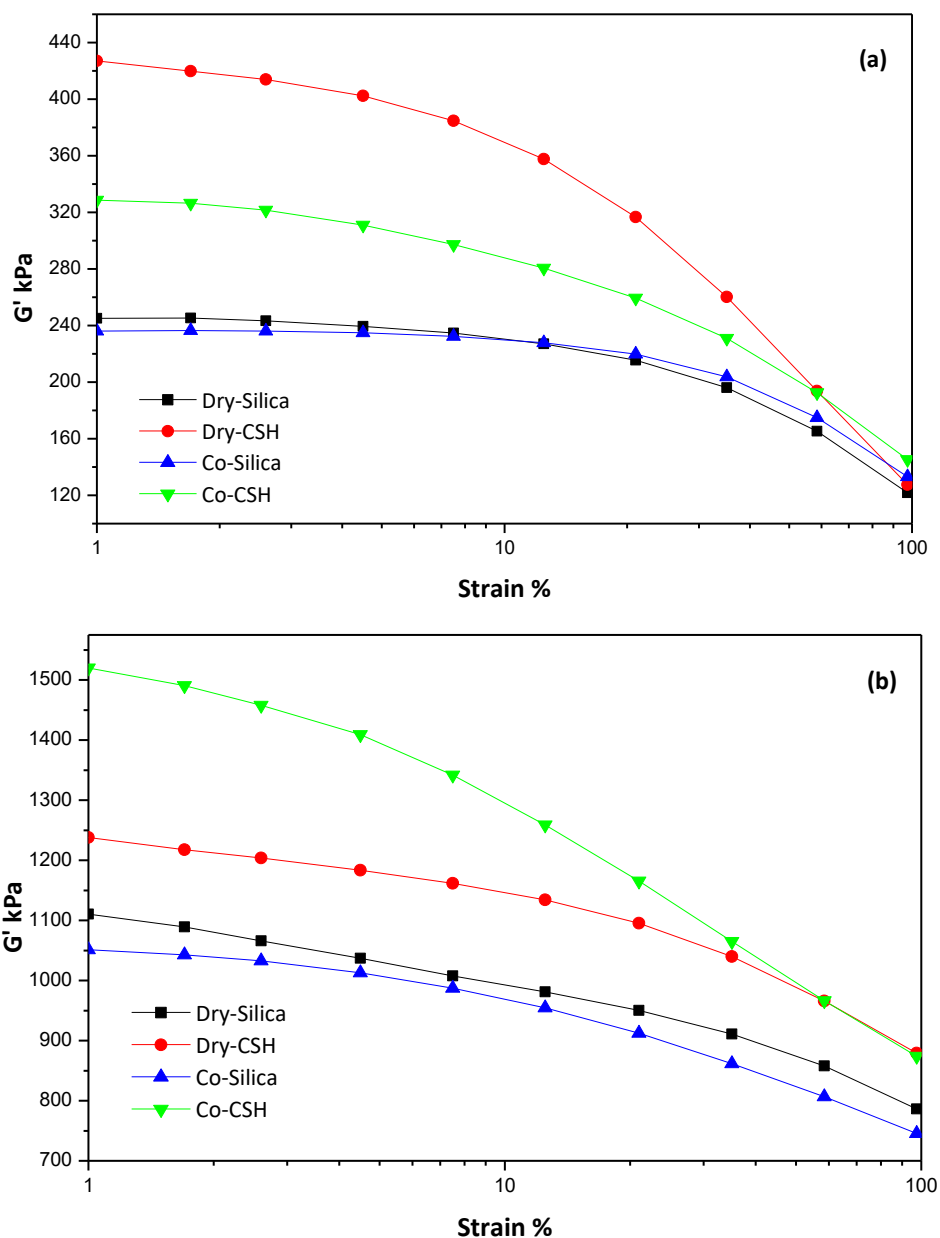


**Figure 6.** Storage modulus vs strain of (a) unvulcanized (b) vulcanized compounds.

Compounds	Dry-Silica	Dry-CSH	Co-Silica	Co-CSH
Payne Effect ( $\Delta G = G'_{0} - G'_{\infty}$ )				
Unvulcanized	123.23	299.56	103.06	183.40
Vulcanized	324.06	359.09	305.66	646.22

**Table 6.** Payne effect of unvulcanized and vulcanized compounds.

The effect of strain amplitude on the  $\tan \delta$  of unvulcanized and vulcanized compounds is shown in Fig. 7.  $\tan \delta$  is the ratio of loss modulus ( $G''$ ) to storage modulus ( $G'$ ). For a viscoelastic material, the  $G'$  measures the stored energy and represents the elastic portion, while  $G''$  represents the energy dissipated as heat (viscous portion) and depend on the rates of filler network breakdown and reformation due to the strain amplitudes [49]. In the unvulcanized compounds at low and intermediate strains, the  $\tan \delta$  remained constant then increased sharply with increasing strains and reached at highest value at high strain amplitude. At low strains, the filler network is capable to reform after deformation and the viscous polymer is stabilized by the filler network, hence a low hysteresis was observed. While at high strain, filler network is broken down and not able to reform in the time frame of dynamic measurement, so polymer chains are no more stabilized by the filler and show more viscous behavior, hence a high hysteresis was observed. It was observed that the two silica compounds have almost same behavior, while the two hybrids showed quite different behavior. The Co-CSH compound showed higher hysteresis than the silica compounds. It can be explained as the hysteresis is resulted due to filler breakdown, so the disruption of a strong filler network during straining dissipates more energy. Furthermore, the hysteresis for Co-CSH compounds was higher than Dry-CSH at low strain but lower at high strain amplitude. This is due to the fact that after the breakdown of filler network, Dry-CSH showed more viscous behavior while the viscous behavior of the Co-CSH was stabilized by the higher filler-polymer interaction which is in agreement with the results of storage modulus obtained through strain sweep. For a given filler, the absolute value of  $\tan \delta$  drastically reduced after the vulcanization which is due to the less viscous nature of the crosslinked polymer matrix. The two silica-filled compounds showed different behavior in vulcanized state. As the co-precipitation method slightly lowered the structure of silica, Dry-Silica compound has higher  $\tan \delta$  at low strain than Co-Silica due to strong filler network of Dry-Silica which build up more heat during cyclic deformation, while at high strains due to improved filler-polymer interactions the Dry-Silica compound has lower  $\tan \delta$  values.



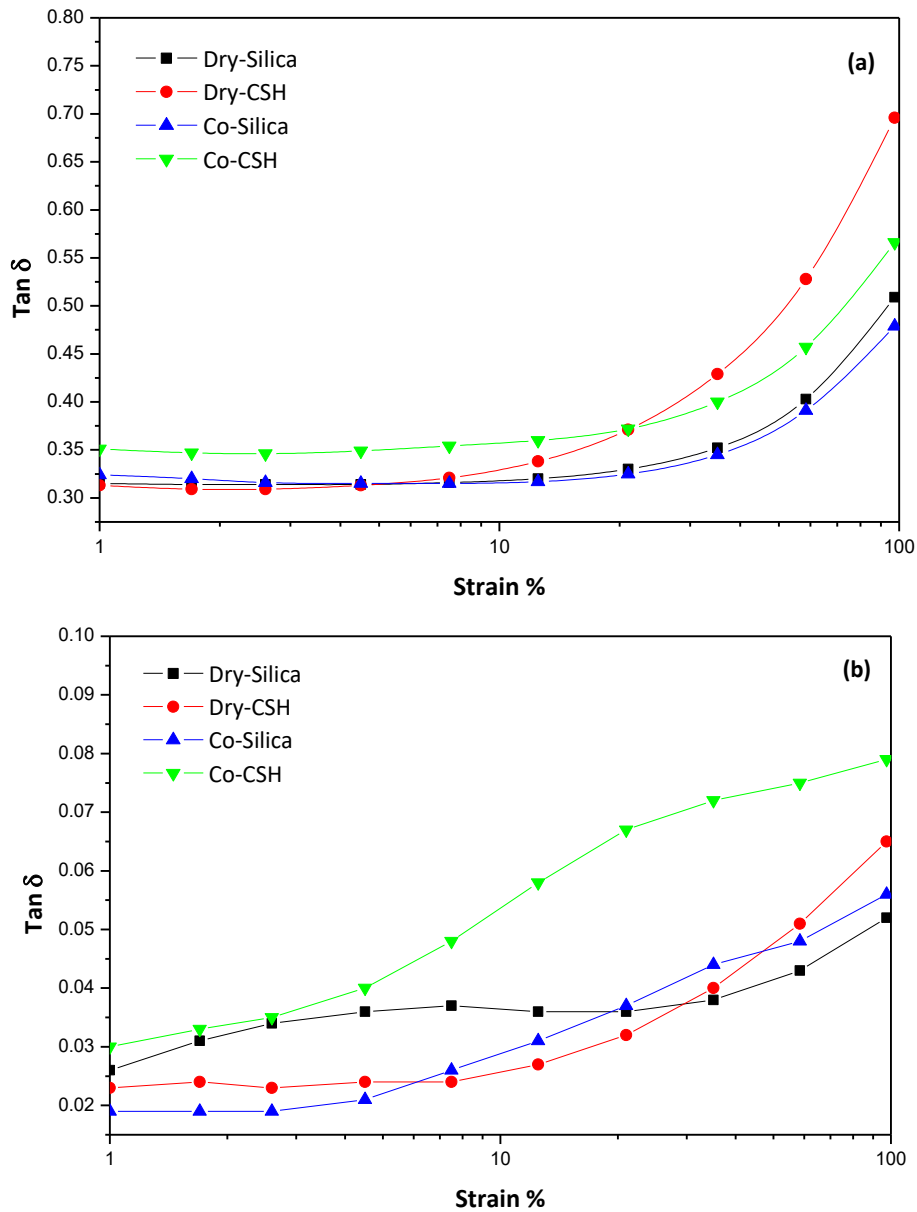


**Figure 7.**  $\tan \delta$  vs strain of (a) unvulcanized (b) vulcanized compounds.

The effect of hybrid as filler on the tensile mechanical properties of the rubber compounds, such as tensile strength (TS), elongation at break (Eb), modulus at 300% strain, was investigated in comparison with reference silica. The effect of the processing method of compounds on these properties was also studied. Modulus at different strain amplitudes, tensile strength, and elongation at break are given in Table 7. A clear difference between the tensile properties of the two hybrids and silica compounds was observed due to the different processing method. Furthermore, tensile properties of the hybrid were quite different than corresponding silica compound. Significant improvement in the tensile properties of the hybrid compound prepared through the co-precipitation was observed and showed very high reinforcement as compared to silica compounds. Two hybrids compounds have very high modulus than silica compounds up to 100% elongation, and then the

modulus of Dry-CSH started to decrease as compared to Co-CSH. The agglomeration of hybrid in dry-mixed compounds lead to poor dispersion in the polymer matrix which resulted in lower tensile strength, elongation at break, and modulus at 300% strain. A higher modulus than silica at low strains up to 200% elongation was due to the higher stiffness of rod-like rigid filler. On the other hand, when the compound was prepared through the co-precipitation, high dispersion of the hybrid in the rubber matrix was obtained. High dispersion of the filler increased the contact area between the anisotropic hybrid filler and the polymer resulted in stronger interfacial interaction between the hybrid filler and polymer, which allowed achieving the improved mechanical properties of the hybrid-filled rubber compounds. Furthermore, this high reinforcing effect of Co-CSH can be assigned to well-known percolation phenomenon of high aspect ratio fillers, which formed a stiffer continuous network of these rod-like hybrid nanoparticles as compared to silica. The tensile behavior of the two silica compounds was slightly different which is due to the different processing method. The Dry-Silica compound showed better reinforcing effect than Co-Silica compound. The Silica was more uniformly distributed through the co-precipitation method, which improved the tensile strength and elongation at break but modulus at 300% strain was lowered. In tire industry, the modulus at 300% elongation is considered as the signature of reinforcement and considered more important than tensile strength and elongation at break. Modulus of the Co-CSH at 300% elongation is much higher than both silica reference compounds which show the enhanced reinforcing ability of the hybrid. The orientation of the high aspect ratio filler particles under strain as well as the formation of strong filler network is attributed to the high level of reinforcement.

Property	Dry-Silica	Dry-CSH	Co-Silica	Co-CSH
Stress 10% (MPa)	0.32	0.50	0.33	0.50
Stress 50% (MPa)	0.95	1.52	0.91	1.38
Stress 100% (MPa)	1.65	2.65	1.51	2.51
Stress 200% (MPa)	4.37	4.95	3.65	6.11
Stress 300% (MPa)	9.28	8.02	8.06	11.07
Elongation at break (%)	504.82	481.61	564.85	523.90
Tensile Strength (MPa)	23.64	17.90	28.97	27.09

**Table 7.** Tensile mechanical properties of the prepared compounds.

### 3.7.2 Effect of Filler Contents

The rubber compounds were prepared at a different loading of hybrid and reference silica to study the effect of filler contents on the properties of the rubber compounds. The compounds were prepared at 20, 30 and 40 PHR of filler loading. The vulcanization parameters are reported in Table 8. Results

showed that the scorch time slightly decreased while the optimum curing time increased with the increase of filler contents. Hence, cure rate index (CRI) representative of vulcanization rate decreased with the increase of filler loading for both hybrid and silica compounds. The decrease of  $T_{S2}$  and increase of  $T_{90}$  with increasing filler contents could be due to the fact that, at higher filler contents more silane coated filler is available which facilitate the early start of the vulcanization process [50]. It can be clearly seen from the  $\Delta M$  values that the crosslink density is high at high filler contents, so the vulcanization process take more time for completion which resulted in high  $T_{90}$  values. For a given loading of filler, the  $T_{S2}$  and  $T_{90}$  for the hybrid were lower while CRI was higher than the respective reference silica compound. Hence, hybrid compounds showed a higher rate of vulcanization than silica compounds. Two other important characteristics of vulcanization process i.e. minimum ( $M_L$ ) and maximum ( $M_H$ ) torques also showed an increasing trend with the increase of filler loading in both silica and hybrid compounds. As the  $M_L$  is indicative of the effective viscosity of the unvulcanized compounds, at high filler contents the viscosity of the unvulcanized compounds increases which resulted in high  $M_L$  values. A high  $M_H$  value at high filler content shows an increase of crosslinking with the increase of filler contents. This is also clear from the value of  $\Delta M$ , which increases with the increase of filler loading showing an increasing degree of crosslinking. The formation of crosslink between the filler and polymer through the coupling agent lead to the enhancement in crosslink density. At high filler loading, more silane is available for polymer-filler crosslinking, which resulted in increased crosslink density of the compounds. The crosslinking density of the hybrid is higher than silica compounds and this effect is more pronounced at high filler loading.

The effect of filler loading on the dynamic mechanical properties of the rubber compounds is summarized in Table 8. Both  $G'$  and Payne effect increase with the increase of filler contents in silica as well as in hybrid compounds. This increase is due to the formation of increased filler network. The inter-particle distances decrease with the increase of filler contents and hence increased the possibility of the formation of the filler network. The hybrid showed higher  $G'$  and Payne effect than respective silica compounds and effect is more pronounced at high filler contents which are attributed to the high aspect ratio of the hybrid particles which formed more stronger filler-network than silica. The  $\tan \delta$  values also increase with the increase of filler contents. As the  $\tan \delta$  represents the amount of energy dissipation during straining, at high filler loading, a strong filler network is formed. Therefore, the disruption of increased filler network during the straining dissipates more energy.

Parameter	Silica-20	Silica-30	Silica-40	CSH-20	CSH-30	CSH-40
<i>Vulcanization parameters</i>						
T <sub>5</sub> 2 (min)	1.45	1.5	1.49	1.22	1.21	1.14
T <sub>90</sub> (min)	3.01	3.41	3.42	2	2.43	2.72
CRI (min <sup>-1</sup> )	64.10	52.35	51.81	128.20	81.96	63.29
M <sub>L</sub> (dNm)	0.81	1.32	1.98	0.69	0.88	2.09
M <sub>H</sub> (dNm)	11.83	13.6	16.09	12.15	14.17	19.14
ΔM (dNm)	11.02	12.28	14.11	11.46	13.29	17.05
<i>Dynamic-mechanical properties</i>						
G' (9%) [MPa]	0.66	0.86	1.07	0.68	0.92	1.39
G' (3%) [MPa]	0.69	0.9	1.17	0.73	0.95	1.6
ΔG'(0.5-10) [MPa]	0.28	0.34	0.49	0.25	0.44	0.98
Tan δ (9%)	0.06	0.047	0.086	0.087	0.089	0.122
Tan δ (3%)	0.064	0.06	0.097	0.089	0.091	0.119
<i>Tensile mechanical properties</i>						
Stress 10% (MPa)	0.32	0.38	0.41	0.38	0.5	0.61
Stress 50% (MPa)	0.94	1.02	1.09	1.14	1.38	1.64
Stress 100% (MPa)	1.6	1.71	1.84	2.14	2.51	2.94
Stress 200% (MPa)	3.62	4.29	4.86	5.42	6.08	6.85
Stress 300% (MPa)	7.77	9.15	10.08	9.98	10.94	12.04
Elongation at break (%)	486.89	549.21	562	535.3	523.9	543.46
Tensile Strength (MPa)	20.37	28.92	27.96	25.47	27.09	28.41

**Table 8.** Effect of filler loading on vulcanization parameters, on dynamic mechanical properties and on tensile mechanical properties of prepared compounds.

The effect of filler contents on the tensile mechanical properties of the rubber compounds was investigated. The modulus at different modulus, elongation at break, and tensile strength are summarized in Table 8. It can be clearly seen from the results that the reinforcement increases with the increase of filler contents. The reinforcement imparted by the addition of hybrid is considerably higher than those provided by the respective silica. It is interesting to note that, the compounds prepared with 20 PHR of hybrid showed similar reinforcement as 40 PHR of silica, however considerable improvement in the density of the final compound was observed. In fact, the density of the prepared compounds were measured. For silica at 20, 30 and 40 PHR the density values (g/cm<sup>3</sup>) were respectively 1.054, 1.097 and 1.131. For the compound filled with CSH at 20, 30 and 40 PHR the densities were 1.046, 1.066 and 1.095 respectively. Hybrid compounds showed much lower density as compared to silica-filled rubber compounds, which is due to the lower density of the prepared hybrid than silica. Therefore, the negative effect of high density of silica was minimized by

introducing the hybrid as filler in rubber compounds, in addition to the higher reinforcing effect of the hybrid than silica.

#### 4. Conclusions

A hybrid of CNCs and silica was synthesized and used as reinforcing filler in natural rubber compounds. The CNC/Silica hybrid was prepared by a simple and efficient co-precipitation method using CNCs as a template and the surface was coated with a silica layer. The core-shell structure of the prepared hybrid was confirmed by FESEM and surface area analysis. Silica layer of about 8-10 nm thickness was decorated on the surface of CNCs. The crystallinity of the hybrid was checked by XRD analysis, the crystal structure of the CNCs was preserved however decrease in crystallinity was observed due to the presence of amorphous silica part. TGA analysis demonstrated that the prepared CNC/Silica hybrid contains about 45% of CNCs contents and about 55% of silica contents. The hybrid was incorporated as reinforcing filler in natural rubber using dry-mixing and co-precipitation methods and compared with standard high reinforcing silica used in the tire industry. Vulcanization characteristics, dynamic mechanical and tensile mechanical properties were investigated. The high aspect ratio of rod-like hybrid particles developed not only strong filler network but also strong filler-polymer interactions. The compounds prepared by the co-precipitation method showed the high dispersion of hybrid in the rubber matrix and demonstrated much higher reinforcing effect than dry-mixed hybrid compound and reference silica compound as well. The effect of filler contents of hybrid on the physio-mechanical properties of the prepared compounds was studied and compared with reference silica. It was demonstrated that the compounds prepared with 20 PHR of hybrid showed similar reinforcement as 40 PHR of silica, however significant improvement in the density of the final compound was observed. Based on the obtained results, it was concluded that the hybrid can be used as a potential reinforcing filler in tire tread compounds with higher reinforcement and lower density than tradition silica filler.

#### References

- [1] H. Angellier, S. Molina-Boisseau, A. Dufresne, *Macromolecules* 38 (2005) 9161–9170.
- [2] M. Arroyo, M.A. López-Manchado, B. Herrero, *Polymer (Guildf)*. 44 (2003) 2447–2453.
- [3] M. Castellano, L. Conzatti, G. Costa, L. Falqui, A. Turturro, B. Valenti, F. Negroni, *Polymer (Guildf)*. 46 (2005) 695–703.
- [4] L. Bokobza, J.P. Chauvin, *Polymer (Guildf)*. 46 (2005) 4144–4151.
- [5] A. Ansarifar, L. Wang, R.J. Ellis, Y. Haile-Meskel, *J. Appl. Polym. Sci.* 119 (2011) 922–928.
- [6] T.A. Vilgis, G. Heinrich, *Macromolecules* 27 (1994) 7846–7854.

- [7] W.M. Hess, W.K. Klamp, *Rubber Chem. Technol.* 56 (1983) 390–417.
- [8] R.R. Heinz Esch, Udo Görl, Robert Kuhlmann, *Precipitated Silicas*, 0647591, 1995.
- [9] N. Rattanasom, S. Prasertsri, T. Ruangritnumchai, *Polym. Test.* 28 (2009) 8–12.
- [10] H. Peng, L. Liu, Y. Luo, X. Wang, D. Jia, *Polym. Compos.* 30 (2009) 955–961.
- [11] K.W. Stöckelhuber, A. Das, R. Jurk, G. Heinrich, *Polymer (Guildf)*. 51 (2010) 1954–1963.
- [12] J.P.F. Lagerwall, C. Schütz, M. Salajkova, J. Noh, J. Hyun Park, G. Scalia, L. Bergström, *NPG Asia Mater.* 6 (2014) e80.
- [13] N. Lin, J. Huang, A. Dufresne, *Nanoscale* 4 (2012) 3274.
- [14] V. Favier, H. Chanzy, J.Y. Cavaille, *Macromolecules* 28 (1995) 6365–6367.
- [15] K. Gopalan Nair, A. Dufresne, N.M. Behavior, *Biomacromolecules* 4 (2003) 666–674.
- [16] A. Bendahou, H. Kaddami, A. Dufresne, *Eur. Polym. J.* 46 (2010) 609–620.
- [17] K. Tashiro, M. Kobayashi, *Polymer (Guildf)*. 32 (1991) 1516–1526.
- [18] D. Barana, A. Salanti, M. Orlandi, D.S. Ali, L. Zoia, *Ind. Crops Prod.* 86 (2016) 31–39.
- [19] A.P. Wight, M.E. Davis, *Chem. Rev.* 102 (2002) 3589–3614.
- [20] F. Hoffmann, M. Cornelius, J. Morell, M. Fröba, *Angew. Chemie - Int. Ed.* 45 (2006) 3216–3251.
- [21] C. Sanchez, P. Belleville, M. Popall, L. Nicole, *Chem. Soc. Rev.* 40 (2011) 696.
- [22] C. Sanchez, B. Julián, P. Belleville, M. Popall, *J. Mater. Chem.* 15 (2005) 3559.
- [23] S. Yano, *Polymer (Guildf)*. 35 (1994) 5565–5570.
- [24] R.A. Zoppi, M.C. Gonçalves, *J. Appl. Polym. Sci.* 84 (2002) 2196–2205.
- [25] K. Tanaka, H. Kozuka, *J. Mater. Sci.* 40 (2005) 5199–5206.
- [26] R.S. Gill, M. Marquez, G. Larsen, *Microporous Mesoporous Mater.* 85 (2005) 129–135.
- [27] S. Sequeira, D. V. Evtuguin, I. Portugal, *Polym. Compos.* 30 (2009) 1275–1282.
- [28] S. Sequeira, D. V. Evtuguin, I. Portugal, A.P. Esculcas, *Mater. Sci. Eng. C* 27 (2007) 172–179.
- [29] H.S. Barud, R.M.N. Assunção, M.A.U. Martines, J. Dexpert-Ghys, R.F.C. Marques, Y. Messaddeq, S.J.L. Ribeiro, in: *J. Sol-Gel Sci. Technol.*, Springer US, 2008, pp. 363–367.
- [30] M.A. Tshabalala, P. Kingshott, M.R. VanLandingham, D. Plackett, *J. Appl. Polym. Sci.* 88 (2003) 2828–2841.
- [31] M. Abdelmouleh, S. Boufi, M.N. Belgacem, A. Dufresne, A. Gandini, *J. Appl. Polym. Sci.* 98 (2005) 974–984.
- [32] B. Ding, C. Li, Y. Hotta, J. Kim, O. Kuwaki, S. Shiratori, *Nanotechnology* 17 (2006) 4332–4339.
- [33] X. Chen, Y. Liu, H. Lu, H. Yang, X. Zhou, J.H. Xin, *Cellulose* 17 (2010) 1103–1113.
- [34] J. Alongi, M. Ciobanu, G. Malucelli, *Cellulose* 18 (2011) 167–177.

- [35] M. Kaushik, H.M. Friedman, M. Bateman, A. Moores, *RSC Adv.* 5 (2015) 53207–53210.
- [36] M. Rezayat, R.K. Blundell, J.E. Camp, D.A. Walsh, W. Thielemans, *ACS Sustain. Chem. Eng.* 2 (2014) 1241–1250.
- [37] X. Wu, C. Lu, Z. Zhou, G. Yuan, R. Xiong, X. Zhang, *Environ. Sci. Nano* 1 (2014) 71.
- [38] W.H. Dokter, I.I.M. Tjiburg, *Precipitated Silica, a Process to Make It, and Its Use*, WO2001007364 A1, 2001.
- [39] J. Song, G. Fu, Q. Cheng, Y. Jin, *Ind. Eng. Chem. Res.* 53 (2014) 708–714.
- [40] R.C. Schroden, C.F. Blanford, B.J. Melde, B.J.S. Johnson, A. Stein, *Chem. Mater.* 13 (2001) 1074–1081.
- [41] S.R. and W. FX, in: *Spectrom. Identif. Org. Compd.*, 2010, pp. 71–143.
- [42] M. Kacuráková, A.C. Smith, M.J. Gidley, R.H. Wilson, *Carbohydr. Res.* 337 (2002) 1145–53.
- [43] E.M. Dannenberg, *Rubber Chem. Technol.* 48 (1975) 410–444.
- [44] S.-S. Choi, B.-H. Park, H. Song, *Polym. Adv. Technol.* 15 (2004) 122–127.
- [45] M.A. Kader, C. Nah, *Polymer (Guildf)*. 45 (2004) 2237–2247.
- [46] C.H. Chen, J.L. Koenig, J.R. Shelton, E.A. Collins, *Rubber Chem. Technol.* 55 (1982) 103–115.
- [47] R.M. Russell, T.D. Skinner, A.A. Watson, *Rubber Chem. Technol.* 42 (1969) 418–440.
- [48] J. Fröhlich, W. Niedermeier, H.D. Luginsland, *Compos. Part A Appl. Sci. Manuf.* 36 (2005) 449–460.
- [49] M.A. Meyers, K. Chawla, *Mechanical Behavior of Materials*, Cambridge University Press, 2009.
- [50] W. Bai, K. Li, *Compos. Part A Appl. Sci. Manuf.* 40 (2009) 1597–1605.